



Short Communication

Co-registration of radiotherapy planning and recurrence scans with different imaging modalities in head and neck cancer



Morten Horsholt Kristensen^{a,*}, Christian Rønn Hansen^{b,c,d}, Ruta Zukauskaitė^e, Jørgen Johansen^e, Eva Samsøe^{f,g}, Christian Maare^f, Anne Ivalu Sander Holm^h, Jesper Grau Eriksen^{a,h}

^a Dept. of Experimental Clinical Oncology, Aarhus University Hospital, Palle Juul-Jensens Boulevard 99, 8200 Aarhus N, Denmark

^b Laboratory of Radiation Physics, Odense University Hospital, Sdr. Boulevard 29, 5000 Odense C, Denmark

^c Dept. of Clinical Research, University of Southern Denmark, Sdr. Boulevard 29, 5000 Odense C, Denmark

^d Danish Centre for Particle Therapy, Aarhus University Hospital, Palle Juul-Jensens Boulevard 25, 8200 Aarhus N, Denmark

^e Dept. of Oncology, Odense University Hospital, Sdr. Boulevard 29, 5000 Odense C, Denmark

^f Dept. of Oncology, Herlev Hospital, Borgmester Ib Juuls Vej 1, 2730 Herlev, Denmark

^g Dept. of Oncology, Zealand University Hospital, Næstved Sygehus, Rådmandsengen 5, 4700 Næstved, Denmark

^h Dept. of Oncology, Aarhus University Hospital, Palle Juul-Jensens Boulevard 99, 8200 Aarhus N, Denmark

ARTICLE INFO

Keywords:

Validation

Deformable Image Registration

Head and neck squamous cell carcinoma

Failure

CT-MRI

ABSTRACT

MRI (magnetic resonance imaging) scans are frequently used in follow-up after radiotherapy for head and neck cancer. With the overall aim of enabling MRI-based pattern of failure analysis, this study evaluated the accuracy of recurrence MRI (rMRI) deformable co-registration with planning CT (computed tomography)-scans (pCT). Uncertainty of anatomical changes between pCT and rMRI was assessed by similarity metric analyses of co-registered image structures from 19 patients. Average mean distance to agreement and Dice similarity coefficient performed adequately. Our findings provide proof of concept for reliable co-registration of pCT and rMRI months to years apart for MRI-based pattern of failure analysis.

1. Introduction

Failures in head and neck squamous cell carcinoma (HNSCC) most often occur locally within 18 months from primary treatment [1–3]. Optimization of treatment requires knowledge of the pattern of failure in HNSCC. Applying deformable image registration (DIR) of the planning CT (computed tomography)-scans (pCT) and recurrence scans enables analysis of the pattern of failure. The volume, point of origin or trigger of the recurrence can be related to the original targets and dose plan, allowing quality assurance of target definitions and setup margins. CT-based pattern of failure analyses have revealed that the majority of recurrences occur in relation to the original high-dose target after primary radiotherapy (RT) [2,4]. A valid method is needed for MRI (magnetic resonance imaging)-based DIR between pCT and recurrence MRI (rMRI) in order to conduct pattern of failure analyses of patients where MRI-scans were used in the follow-up setting.

Deformable image registration between scans of different modalities are frequently utilized in RT planning [5]. If a patient is suspected of

having a loco-regional recurrence after primary RT, a scan of the suspected area is usually performed. Traditionally, this involves a CT-scan, however, in some instances, MRI is preferred due to the higher contrasts of soft tissues and thus recommended by national guidelines for certain anatomical regions in the head and neck [6].

Co-registration method of planning-CT to recurrence-CT scans have been validated with mean surface distances ranging from 1 to 3 mm for DIR and between 1 and 1.5 mm for re-delineation uncertainty [7]. Since most recurrence scans traditionally are CT-based, most studies of recurrences/failures have not included MRI-based scans [2,4,8,9]. Other studies have included MRI, however to our knowledge, time-staggered DIR of CT-MRI has not previously been validated [10–12].

The time interval between primary RT and recurrence can contribute to a significant change in anatomy. Changes may include atrophy of normal tissues (e.g. parotid glands) as a late effect of irradiation, weight loss, fibrosis, where stiffness prevents optimal extension of the neck or other posture changes, the presence of a primary tumor on pCT, and a recurrent tumor on the recurrence scan [13,14]. These factors are time-

* Corresponding author.

E-mail address: mortenhorsholt@oncology.au.dk (M.H. Kristensen).

<https://doi.org/10.1016/j.phro.2022.06.012>

Received 11 February 2022; Received in revised form 24 June 2022; Accepted 27 June 2022

Available online 30 June 2022

2405-6316/© 2022 The Authors. Published by Elsevier B.V. on behalf of European Society of Radiotherapy & Oncology. This is an open access article under the CC BY-NC-ND license (<http://creativecommons.org/licenses/by-nc-nd/4.0/>).

Table 1

Mean values of metric analyses of five regions of interest including the mean volume (cm^3) of the structures. ROI: Region of interest; Man: Manual delineation; DIR: Deformable image registration; SD: Standard deviation; HD: Hausdorff distance (mm); MDA: Mean distance to agreement (mm); DICE: Dice similarity coefficient (index).

		Volume, cm^3		HD Man, mm		HD DIR, mm		MDA Man, mm		MDA DIR, mm		DICE Man		DICE DIR	
		Mean	SD	Mean	SD	Mean	SD	Mean	SD	Mean	SD	Mean	SD	Mean	SD
ROI	Parotid gland, right	25.5	10.8	9.5	2.8	12.9	4.6	1.1	0.5	2.2	0.7	0.84	0.06	0.73	0.08
	Parotid gland, left	25.2	9.8	9.8	4.2	14.4	5.0	1.1	0.4	2.2	0.6	0.85	0.06	0.73	0.08
	Maxillar sinus, right	15.0	3.8	5.7	2.8	8.6	4.1	0.6	0.2	1.4	0.6	0.90	0.04	0.80	0.08
	Maxillar sinus, left	13.8	3.0	4.8	1.8	7.7	3.2	0.5	0.2	1.2	0.6	0.91	0.03	0.83	0.06
	Spinal cord, C1-C7	9.1	2.6	5.0	2.9	9.2	5.5	0.7	0.5	1.3	0.6	0.82	0.09	0.73	0.09

dependent between the original and the failure scans and contribute to the uncertainty of the intended co-registration of the two scans, since anatomy may have changed.

MRI provides superior soft-tissue contrast compared to CT, and artefacts related to dental implants are different and often less pronounced [15,16]. However, when aiming to co-register the two scans, the modality difference might cause additional uncertainty.

This study aimed to evaluate the precision of DIR between scans of different modalities and staggered in time for HNSCC patients, which could provide the foundation for larger cohorts of failure analysis if a shift toward more frequent use of MRI-based recurrence scans in the follow-up setting after HNSCC.

2. Materials and methods

The cohort for this study consisted of 20 patients with loco-regional recurrence of squamous cell carcinoma of the oral cavity, pharynx or larynx. The patients were treated in a well-defined cohort of patients within the DAHANCA 19 study (2007–12). Patients received standard radiotherapy according to DAHANCA guidelines with IMRT [17]. Patients were included if the failure was diagnosed within the five-year follow-up period. Included in the present study were patients solely with MRI-based recurrence scans (i.e. no PET-CT or CT scans upon recurrence) in which the recurrence volume was visible. Treatment pCTs including original structure sets along with MRI-scans performed at recurrence before any surgical or oncologic intervention were identified and transferred to the secure DICOM Collaboration system (DcmCollab, Odense University Hospital, Denmark) [18,19]. Both pCTs and rMRIs were imported to MIM software (Cleveland, USA, version 7.2) in which delineation of regions of interest (ROIs), co-registration, and analysis for measures of uncertainty were performed.

To test the feasibility of DIR between the two different scanning modalities at two different time points, three regions of interest (ROIs) were selected for validation: spinal cord (from the oval foramen/tip of dens axis C1 to the superior border of corpus vertebrae of C7), bilateral parotid glands, and bilateral cavities of maxillary sinuses (including mucosa).

Deformable image registration was successful for 19 out of 20 patients. The median time from the end of RT to diagnosed failure was eight (range 2–43) months. For detailed tumor and patient characteristics, see [Supplementary Table 1](#).

The pCTs were all conducted with a source potential of 120 kV and a slice thickness between two ($n = 3$) and three ($n = 16$) mm. Delineation of structures was conducted on T1 weighted rMRI sequences for all cases. Median slice thickness for rMRI was 4.4 (range 0.9–7.5) mm. For specifications regarding techniques of the rMRIs used, manufacturer and model of the scans, see [Supplementary Table 2](#).

Ethics statement: Patients in the DAHANCA 19 (NCT00496652) study gave consent for the use of patient material (including scans) for future research.

2.1. Manual delineation

To evaluate the uncertainty of ROI delineation, a head and neck radiation oncologist delineated the above-mentioned ROIs on the rMRI in MIM. Problematic cases were discussed with senior colleagues. After an interval of a minimum of one month, the ROIs were re-delineated by the same observer without guidance from the first delineation session. This resulted in rMRIs with two structure sets available for analyses of intraobserver variance.

For one of the patients, the rMRI was conducted to identify a recurrence in the posterior nasal cavity and nasopharynx, hence, only the maxillary sinuses could be used for comparison. For another patient, the MRI did not include the entire volume of the maxillae, hence, only the spinal cord and parotids were used for comparison. The remaining 17 rMRIs included all five ROIs for comparison.

2.2. Time and modality factor

Uncertainties of MRI-CT DIR were both a measure of the uncertainty of the potential anatomical changes over time from planning RT to recurrence and of the discrepancies in the different modalities of the two scans. The pCTs included the original structure sets. If a structure set on the pCT contained the ROIs used for the analyses, these would be evaluated and used. If they were not present in the original structure set or the structures would not adhere to guidelines, contouring or corrections of existing structures would be added to the ROI in the pCT.

To co-register the scans, first an automated rigid assisted alignment of the pCT and rMRI (including the first set of contoured ROIs from the manual delineation) was performed. These fused scans were deformable registered using multi-modality setting. For details on co-registration see [Supplementary S1](#). The volumes of the ROIs were extracted from the pCTs.

2.3. Measures of similarity

Three metrics were utilized for the evaluation of contour similarities: Dice similarity coefficient (DICE), Hausdorff distance (HD), and mean distance to agreement (MDA). These were applied per patient to analyse the uncertainties. For details regarding DICE, HD and MDA, see [Supplementary material S2](#).

From the rMRIs including the two sets of delineated ROIs, the metrics were applied to evaluate the uncertainty of the manual delineation (intraobserver variation). From the pCTs including the DIR-propagated ROIs from the rMRIs, the time and modality factor uncertainties were calculated. In total, 273 ROIs were considered and analysed.

3. Results

Mean MDA for DIR ranged between 1.2 and 2.2 mm, corresponding to average DICE values between 0.73 and 0.83. The highest levels of uncertainty were found for the parotid glands, and the best match for both the manual delineation and DIR were the maxillary sinuses. Mean values of HD, MDA and DICE both for the manual delineation and DIR

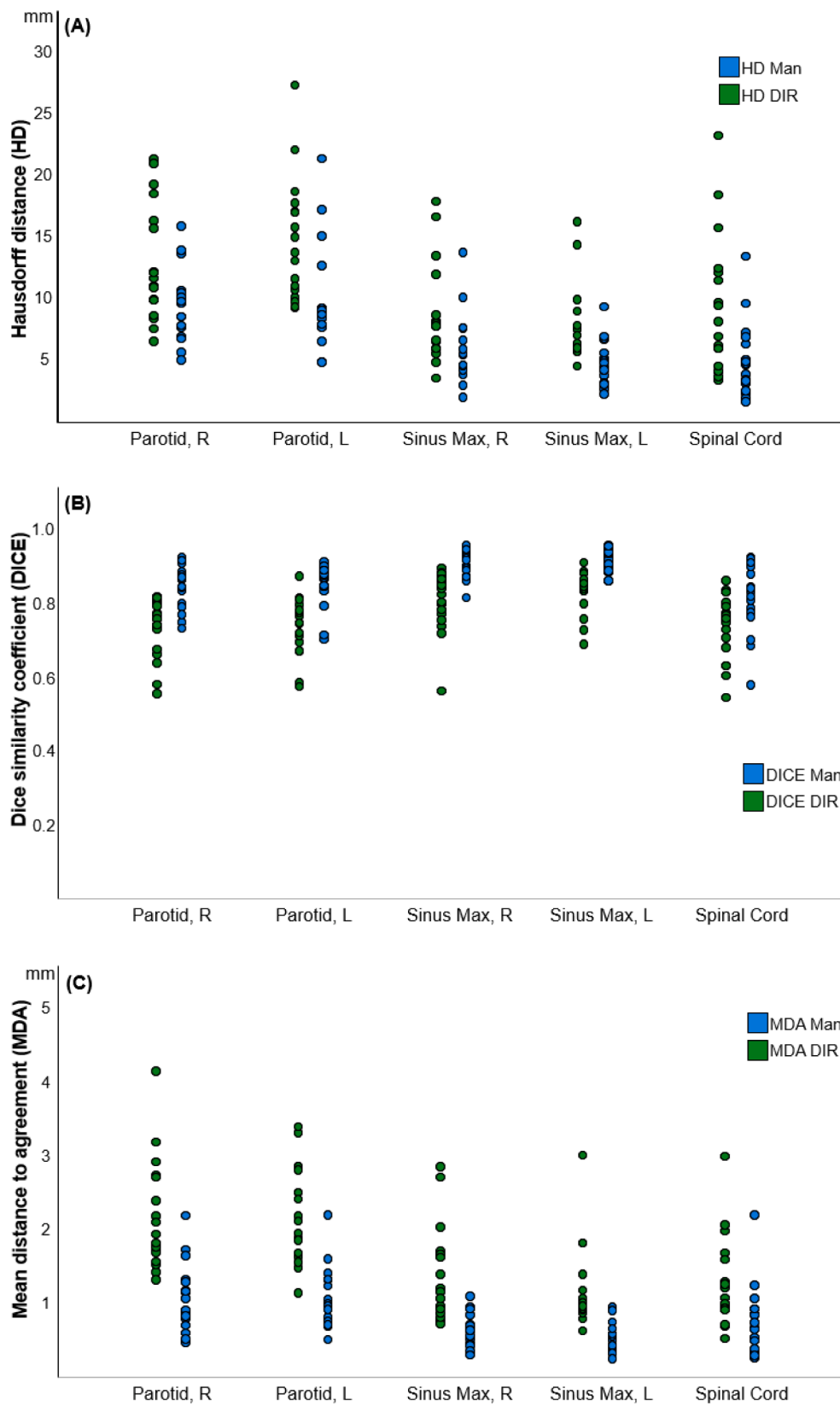


Fig. 1. Strip plots of metrics for DIR and Man. Strip plots of values of the metric analyses for each region of interest (x-axis): manual delineation (blue) and deformable image registration (green). A: Hausdorff distances in mm (y-axis); B: Dice similarity coefficient index value (y-axis); C: Mean Distance to Agreement in mm (y-axis); Man: Manual delineation; DIR: Deformable image registration; HD: Hausdorff Distance; DICE; Dice similarity coefficient; MDA: Mean Distance to Agreement.

for each organ are shown in Table 1. All metric values for each ROI were normally distributed.

Overall, the comparisons between the two sets of manual delineations on the rMRIs performed superior to the DIR between time-staggered pCT and rMRI (lowest HD and MDA; highest DICE). For the DIR, the parotid glands were the ROIs with the largest uncertainty, whereas the maxillary sinuses performed best. Fig. 1 contains strip plots of the metric analyses of the DIR and manual delineation.

4. Discussion

This study investigated intraobserver variance and the uncertainty of time-staggered DIR between pCT and rMRI in head and neck cancer to test whether this method would allow for pattern of failure analysis using scans of different modality. The study showed average uncertainties below 2.2 mm (MDA) and DICE values larger than 0.73 for time-separated DIR between CT and MRI scans. The mean HD ranged between 7.7 mm (left maxillary sinus) and 14.4 mm (left parotid gland). Large HDs were found both for manual delineation and DIR for parotid glands, most pronounced for DIR. This uncertainty may be explained by the difference in soft tissue contrast between MRI and CT scans, where both the superficial/anterior extent and the extension into the lateral pharyngeal space appear very different with the two techniques. The pockets of mean greatest dissimilarity (high mean HD) were found among the parotid glands, which also were the ROIs with the largest volumes. This association between larger volumes and larger variance is consistent with previous findings [7].

When comparing our results to the recommended tolerance uncertainties formulated by K. Brock et al. [20], the majority (95%) of MDAs for DIR were within tolerance, defined by the maximum voxel dimension ($\approx 2\text{--}3$ mm) for the pCTs and for the rMRIs ($\approx 0.9\text{--}7.5$ mm). For DICE, the lower tolerated index value was set to 0.8 by the American Association of Physicists in Medicine's task force wherein our study, only DIR for the maxillary sinuses had indexes approaching the tolerance level (70% of the DIR values) [20]. However, the purpose of this study was to evaluate the uncertainty of the DIR method for pattern of failure analyses and not for precise tumour contouring for clinical treatment.

In the most ideal setting, HD would be zero when comparing the two structure sets on the rMRI. However, delineation is a series of choices and despite HDs between 5 and 10 mm, DICE for the intraobserver variability (0.82–0.91) in this study was comparable with other studies [7,21].

In our study, the contour sets from the original pCTs were co-registered with rMRIs if the ROI was present in the pCT. The original contour sets contained contours from many different radiation oncologists and despite a tradition for using common, national delineation guidelines in Denmark, some interobserver variability must be assumed [22]. The disadvantage of comparing contours from different observers is the risk of larger uncertainty. In contrary, the advantage is that the generalisability is strengthened, since the DIR performed with acceptable overall accuracy despite multiple contour set comparisons for the parotid glands and the spinal cord.

The reason for selecting the three ROIs in this study were to evaluate the uncertainty of structures with longitudinal extension in the area where loco-regional recurrences can occur (spinal cord) and include potential deformation uncertainties of both bony (maxillary sinuses) and soft tissue (parotid glands), more prone to atrophy as a late effect of RT. We found that, overall, the maxillary sinus performed best with the lowest uncertainties. This might be due to the fact, that none of the pCTs included this ROI, hence delineation was performed by the same observer for all three sets of contours in this study. Another potential contributing factor could be that the maxillary sinus is an aerial cavity in a bony structure and therefore more precisely defined by contrast even on a T1-weighted MRI scan.

Since the rMRIs in our study are around 10 years old (conducted

between 2009 and 2013), the quality of the scans are somewhat inferior to the capabilities of modern MRI scans, however, the scan sequence used is still the standard for OAR delineation, so improvements are primarily in the better geometric resolution and signal to noise ratio. Future studies may find more accurate volume overlay on DIR, with the presumed enhanced technical quality.

For the purpose of failure analyses, comparing scans of different modalities in HNSCC over time, the uncertainties are acceptable, hence establishing the foundation for future studies to include patients irrespective of the modality of the recurrence scans.

Declaration of Competing Interest

The authors declare that they have no known competing financial interests or personal relationships that could have appeared to influence the work reported in this paper.

Appendix A. Supplementary data

Supplementary data to this article can be found online at <https://doi.org/10.1016/j.phro.2022.06.012>.

References

- [1] Overgaard J, Hansen HS, Specht L, Overgaard M, Grau C, Andersen E, et al. Five compared with six fractions per week of conventional radiotherapy of squamous-cell carcinoma of head and neck: DAHANCA 6&7 randomised controlled trial. *Lancet* 2003;362:933–40. [https://doi.org/10.1016/S0140-6736\(03\)14361-9](https://doi.org/10.1016/S0140-6736(03)14361-9).
- [2] Zukauskaitė R, Hansen CR, Grau C, Samsøe E, Johansen J, Petersen JBB, et al. Local recurrences after curative IMRT for HNSCC: Effect of different GTV to high-dose CTV margins. *Radiother Oncol* 2018;126:48–55. <https://doi.org/10.1016/j.radonc.2017.11.024>.
- [3] Pagh A, Grau C, Overgaard J. Failure pattern and salvage treatment after radical treatment of head and neck cancer. *Acta Oncol* 2016;55:625–32. <https://doi.org/10.3109/0284186X.2015.1117136>.
- [4] Due AK, Vogeliuss IR, Aznar MC, Bentzen SM, Berthelsen AK, Korreman SS, et al. Recurrences after intensity modulated radiotherapy for head and neck squamous cell carcinoma more likely to originate from regions with high baseline [18F]-FDG uptake. *Radiother Oncol* 2014;111:360–5. <https://doi.org/10.1016/j.radonc.2014.06.001>.
- [5] Daisne JF, Duprez T, Weynand B, Lonnet M, Hamoir M, Reyckler H, et al. Tumor volume in pharyngolaryngeal squamous cell carcinoma: Comparison at CT, MR imaging, and FDG PET and validation with surgical specimen. *Radiology* 2004;233:93–100. <https://doi.org/10.1148/radiol.2331030660>.
- [6] Jensen K, Al-Farra G, Dejanovic D, Eriksen JG, Loft A, Hansen CR, et al. Imaging for target delineation in head and neck cancer radiotherapy. *Semin Nucl Med* 2021;51:59–67. <https://doi.org/10.1053/j.semnuclmed.2020.07.010>.
- [7] Zukauskaitė R, Brink C, Hansen CR, Bertelsen A, Johansen J, Grau C, et al. Open-Source-System für die deformierbare Bildregistrierung von Planungs- und Rezidiv-CT-Datensätzen: Validierung im Kopf-Hals-Bereich. *Strahlenther Onkol* 2016;192:545–51. <https://doi.org/10.1007/s00066-016-0998-4>.
- [8] Due AK, Vogeliuss IR, Aznar MC, Bentzen SM, Berthelsen AK, Korreman SS, et al. Methods for estimating the site of origin of locoregional recurrence in head and neck squamous cell carcinoma. *Strahlenther Onkol* 2012;188:671–6. <https://doi.org/10.1007/s00066-012-0127-y>.
- [9] Shakam A, Scrimger R, Liu D, Mohamed M, Parliament M, Field GC, et al. Dose-volume analysis of locoregional recurrences in head and neck IMRT, as determined by deformable registration: A prospective multi-institutional trial. *Radiother Oncol* 2011;99:101–7. <https://doi.org/10.1016/j.radonc.2011.05.008>.
- [10] Nissi L, Suilamo S, Kytö E, Vaittinen S, Irjala H, Minn H. Recurrence of head and neck squamous cell carcinoma in relation to high-risk treatment volume. *Clin Transl Radiat Oncol* 2021;27:139–46. <https://doi.org/10.1016/j.ctro.2021.01.013>.
- [11] Bayman E, Prestwich RJD, Speight R, Aspin L, Garratt L, Wilson S, et al. Patterns of failure after intensity-modulated radiotherapy in head and neck squamous cell carcinoma using compartmental clinical target volume delineation. *Clin Oncol* 2014;26:636–42. <https://doi.org/10.1016/j.clon.2014.05.001>.
- [12] Raktøe SAS, Dehnad H, Raaijmakers CPJ, Braunius W, Terhaar CHJ. Origin of tumor recurrence after intensity modulated radiation therapy for oropharyngeal squamous cell carcinoma. *Int J Radiat Oncol Biol Phys* 2013;85:136–41. <https://doi.org/10.1016/j.ijrobp.2012.02.042>.
- [13] Mohamed ASR, Ruangsikul MN, Awan MJ, Baron CA, Kalpathy-Cramer J, Castillo R, et al. Quality assurance assessment of diagnostic and radiation therapy-simulation CT image registration for head and neck radiation therapy: Anatomic region of interest-based comparison of rigid and deformable algorithms. *Radiology* 2015;274:752–63. <https://doi.org/10.1148/radiol.14132871>.
- [14] Mencarelli A, Van Kranen SR, Hamming-Vrieze O, Van Beek S, Nico Rasch CR, Van Herk M, et al. Deformable image registration for adaptive radiation therapy of head and neck cancer: Accuracy and precision in the presence of tumor changes. *Int J*

- Radiat Oncol Biol Phys 2014;90:680–7. <https://doi.org/10.1016/j.ijrobp.2014.06.045>.
- [15] Becker M, Zaidi H. Imaging in head and neck squamous cell carcinoma: The potential role of PET/MRI. Br J Radiol 2014;87:1–15. <https://doi.org/10.1259/bjr.20130677>.
- [16] Hansen CR, Christiansen RL, Lorenzen EL, Bertelsen AS, Asmussen JT, Gyldenkerne N, et al. Contouring and dose calculation in head and neck cancer radiotherapy after reduction of metal artifacts in CT images. Acta Oncol 2017;56: 874–8. <https://doi.org/10.1080/0284186X.2017.1287427>.
- [17] Hansen CR, Johansen J, Kristensen CA, Smulders B, Andersen LJ, Samsøe E, et al. Quality assurance of radiation therapy for head and neck cancer patients treated in DAHANCA 10 randomized trial. Acta Oncol 2015;54:1669–73. <https://doi.org/10.3109/0284186X.2015.1063780>.
- [18] Brink C, Lorenzen EL, Krogh SL, Westberg J, Berg M, Jensen I, et al. DBCG hypo trial validation of radiotherapy parameters from a National Data Bank versus manual reporting. Acta Oncol 2018;57:107–12. <https://doi.org/10.1080/0284186X.2017.1406140>.
- [19] Westberg J, Krogh S, Brink C, Vogelius IR. A DICOM based radiotherapy plan database for research collaboration and reporting. J Phys Conf Ser 2014;489:1–5. <https://doi.org/10.1088/1742-6596/489/1/012100>.
- [20] Brock KK, Mutic S, McNutt TR, Li H, Kessler ML. Use of image registration and fusion algorithms and techniques in radiotherapy: Report of the AAPM Radiation Therapy Committee Task Group No. 132: Report. Med Phys 2017;44:e43–76. <https://doi.org/10.1002/mp.12256>.
- [21] Chuter R, Prestwich R, Bird D, Scarsbrook A, Sykes J, Wilson D, et al. The use of deformable image registration to integrate diagnostic MRI into the radiotherapy planning pathway for head and neck cancer. Radiother Oncol 2017;122:229–35. <https://doi.org/10.1016/j.radonc.2016.07.016>.
- [22] Jensen K, Friberg J, Hansen CR, Samsøe E, Johansen J, Andersen M, et al. The Danish Head and Neck Cancer Group (DAHANCA) 2020 radiotherapy guidelines. Radiother Oncol 2020;151:149–51. <https://doi.org/10.1016/j.radonc.2020.07.037>.